ISSN 1674-1056
http://cpb.iphy.ac.cn
http://iopscience.iop.org/cpb
中国物理 B
Chinese Physics
中国物理
Chinese Physics B

Rectifying characteristics and solar-blind photoresponse in β-Ga_2O_3/ZnO heterojunctions

Xiao-Fei Ma(马晓菲)

Citation: Chin. Phys. B . 2019, 28(8): 088503. **doi:** 10.1088/1674-1056/28/8/088503
Journal homepage: http://cpb.iphy.ac.cn; http://iopscience.iop.org/cpb

What follows is a list of articles you may be interested in

Ge/Si heterojunction L-shape tunnel field-effect transistors with hetero-gate-dielectric

Cong Li(李聪), Zhi-Rui Yan(闫志蕊), Yi-Qi Zhuang(庄奕琪), Xiao-Long Zhao(赵小龙), Jia-Min Guo(郭嘉敏)
Chin. Phys. B . 2018, 27(7): 078502. **doi:** 10.1088/1674-1056/27/7/078502

Simulation and experimental study of a novel bifacial structure of silicon heterojunction solar cell for high efficiency and low cost

Haibin Huang(黄海宾), Gangyu Tian(田罡煜), Lang Zhou(周浪), Jiren Yuan(袁吉仁), Wolfgang R. Fahrner, Wenbin Zhang(张闻斌), Xingbing Li(李杏兵), Wenhao Chen(陈文浩), Renzhong Liu(刘仁中)
Chin. Phys. B . 2018, 27(3): 038502. **doi:** 10.1088/1674-1056/27/3/038502

Improved high-frequency equivalent circuit model based on distributed effects for SiGe HBTs with CBE layout

Ya-Bin Sun(孙亚宾), Xiao-Jin Li(李小进), Jin-Zhong Zhang(张金中), Yan-Ling Shi(石艳玲)
Chin. Phys. B . 2017, 26(9): 098502. **doi:** 10.1088/1674-1056/26/9/098502

Photodetectors based on junctions of two-dimensional transition metal dichalcogenides

Xia Wei(魏侠), Fa-Guang Yan(闫法光), Chao Shen(申超), Quan-Shan Lv(吕全山), Kai-You Wang(王开友)
Chin. Phys. B . 2017, 26(3): 038504. **doi:** 10.1088/1674-1056/26/3/038504

Simulation study of the losses and influences of geminate and bimolecular recombination on the performances of bulk heterojunction organic solar cells

Zhu Jian-Zhuo, Qi Ling-Hui, Du Hui-Jing, Chai Ying-Chun
Chin. Phys. B . 2015, 24(10): 108501. **doi:** 10.1088/1674-1056/24/10/108501

Rectifying characteristics and solar-blind photoresponse in β-Ga_2O_3/ZnO heterojunctions*

Xiao-Fei Ma(马晓菲), Yuan-Qi Huang(黄元琪), Yu-Song Zhi(支钰崧), Xia Wang(王霞), Pei-Gang Li(李培刚), Zhen-Ping Wu(吴真平)†, and Wei-Hua Tang(唐为华)‡

State Key Laboratory of Information Photonics and Optical Communications & School of Science, Beijing University of Posts and Telecommunications, Beijing 100876, *China*

(Received 23 January 2019; revised manuscript received 3 March 2019; published online 9 July 2019)

Heterojunctions composed of β-Ga_2O_3 and ZnO films are fabricated on sapphire substrates by using the laser molecular beam epitaxy method. The heterojunction possesses excellent rectifying characteristics with an asymmetry ratio over 10^5. Prominent solar-blind photoresponse effect is also observed in the formed heterojunction. The photodetector exhibits a self-powered behavior with a fast response speed (rise time and decay time are 0.035 s and 0.032 s respectively) at zero bias. The obtained high performance can be related to the built-in field driven photogenerated electron-hole separation.

Keywords: Ga_2O_3, solar blind photodetector, heterojunction, self-powered

PACS: 85.60.Gz, 73.40.Lq, 67.30.hr, 71.20.Nr **DOI:** 10.1088/1674-1056/28/8/088503

1. Introduction

Photodetectors which can convert optical signals into electrical signals has received intensive attention due to their promising applications in many fields, including military warning, environmental monitoring, chemical and biological analysis, communication security, *etc*.[1–3] With the development of nanometer technology and microelectronic processes, photodetectors with better performance have been fabricated in different structures.[4–6] However, for the complexity of the process and high cost of materials, the photodetectors cannot be widely used. On the other hand, due to the absorption of deep ultraviolet (DUV) light by ozone sphere, photodetectors operating in a wavelength range of 200 nm–280 nm (so-called solar-blind region) do have the advantages of higher sensitivity and lower false alarm rate. Over the past decade, a large number of wide-bandgap semiconductors such as SiC, AlGaN, MgZnO, and β-Ga_2O_3 have been employed to fabricate solar-blind photodetectors.[7–17] Moreover, photodetectors based on wide-bandgap semiconductors are expected to work in harsh conditions like astronautical exploration, to break through the limitations of the bulky power supply for the commercial DUV photodetector based on vacuum photo-multiplier tubes.

The β-Ga_2O_3 (band gap: $\sim$4.9 eV), as a next-generation wide-bandgap semiconductor, is considered as an ideal candidate for photoelectronic and electronic devices.[18–22] Until now, various types of the β-Ga_2O_3 based solar-blind photodetectors have been investigated, including single crystal, thin film, nanostructure, metal-semiconductor-metal (MSM), heterojunction.[15,19,23–29] Among them, heterojunction structure can efficiently enhance the photogenerated carrier transport by tuning the barrier height and realize carrier multiplication via impacting ionization process under relatively large bias, suggesting its promising application in high performance photodetectors. For instance, ZnO–Ga_2O_3 core–shell nanowire based solar-blind avalanche photodetector was reported by Zhao *et al.* The photodetector shows the highest reported responsivity of 1.3×10^3 A/W with a rise time shorter than 20 μs and a decay time of 42 μs. Moreover, for practical purposes, a heterojunction photodetector based on thin-film type is appealing due to its good adhesion and high reproducibility. To ensure good photodetector performance based on the heterojunctions, materials with smaller lattice mismatch are highly desired. So far, several single crystal substrates (Si, Nb:$SrTiO_3$, Ga:ZnO, SiC) are employed to form heterojunctions with Ga_2O_3 films.[25,30–33] In this study, we deposit ZnO thin films and β-Ga_2O_3 thin films on sapphire substrates orderly to fabricate a vertically structured heterojunction. The photodetector based on the thin-film heterojunction exhibits excellent rectification characteristics and self-powered features.

2. Experiment

The β-Ga_2O_3/ZnO heterojunctions were grown on (0001) *c*-plane sapphire substrates by laser molecular beam epitaxy

*Project supported by the National Natural Science Foundation of China (Grant Nos. 51572033, 61774019, 61704153, and 11404029), the Fund from the State Key Laboratory of Information Photonics and Optical Communications (BUPT), China, and the Fundamental Research Funds for the Central Universities, China.

†Corresponding author. E-mail: zhenpingwu@bupt.edu.cn

‡Corresponding author. E-mail: whtang@bupt.edu.cn

© 2019 Chinese Physical Society and IOP Publishing Ltd

(LMBE) with a KrF laser operating at a wavelength $\lambda =$ 248 nm. The laser energy was about 400 mJ at a frequency of 2 Hz. During the deposition, the chamber was evacuated to a base pressure of 1×10^{-5} Pa. The distance between target and substrate was 50 mm, and the growth temperature was 750 ℃. The ZnO layers were first deposited on Al_2O_3 substrates. The subsequent β-Ga_2O_3 thin films were grown on the surface of ZnO films under the same condition by introducing a shelter to cover part of the ZnO films. A schematic view of the β-Ga_2O_3/ZnO heterojunction device is shown in Fig. 1(a). The film structure was characterized by a Bruker D8 Advance x-ray diffractometer (XRD) using Cu Kα ($\lambda = 1.5405$ Å) radiation. In order to measure the current–voltage (I–V) curves and photoresponse of β-Ga_2O_3/ZnO heterojunctions, Indium electrodes (0.1 mm $\times$ 0.1 mm) were fabricated on both the β-Ga_2O_3 layer and ZnO layer. The I–V characteristic curves of the β-Ga_2O_3/ZnO heterojunctions were measured by Keithley 2450. A low-pressure mercury lamp of 254/365 nm wavelength was employed for the photoresponse measurement.

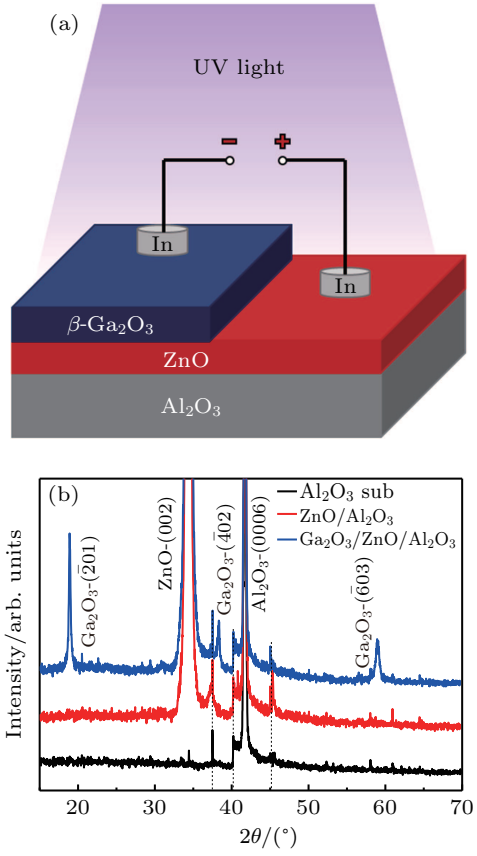


Fig. 1. (a) Schematic diagram of constructed β-Ga_2O_3/ZnO heterojunction, (b) XRD patterns of c-plane Al_2O_3 substrate, ZnO/Al_2O_3, and β-Ga_2O_3/ZnO/Al_2O_3 samples, respectively.

3. Results and discussion

Figure 1(b) shows the XRD patterns of the (0001) sapphire substrate, the ZnO layer, and the β-Ga_2O_3/ZnO heterojunction, respectively. The sapphire (0006) diffraction peak is utilized to calibrate and normalize the patterns. As shown in Fig. 1(b), except for the substrate diffraction peaks, the observed peaks can be indexed to the (002) lattice plane of ZnO (JCPDS Card no. 36-1451). In addition, it is clear that three peaks are observed around 18.8°, 38.2°, and 58.9° corresponding to the $(\bar{2}01)$, $(\bar{4}02)$, and $(\bar{6}03)$ lattice planes of β-Ga_2O_3 (JCPDS Card no. 43-1021) in the pattern of heterojunction. The results indicate that the β-Ga_2O_3 thin films are grown in the $(\bar{2}01)$ orientation.

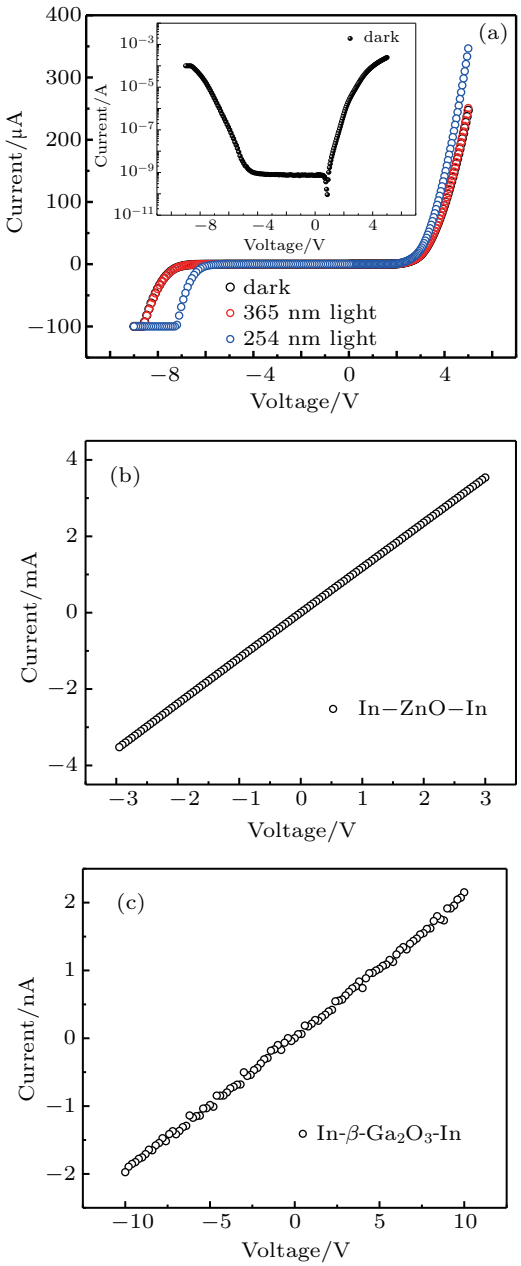


Fig. 2. (a) I–V characteristic curves of the β-Ga_2O_3/ZnO heterojunction in the dark, under 254-nm and 365-nm illuminations, with inset showing I–V curve of heterojunction in the dark in log scale; (b) I–V characteristic curve of the In–ZnO–In structure; (c) I–V characteristic curve of In–β-Ga_2O_3–In structure.

Figure 2(a) shows the I–V characteristic curves of the β-Ga_2O_3/ZnO heterojunction in the dark and under the illumination of 254-nm and 365-nm light, respectively. Here, the

forward bias is set as the current flowing from the ZnO thin film into the β-Ga_2O_3 thin film. The contact between the In–ZnO and the In–β-Ga_2O_3 is confirmed as Ohmic contact by the linear I–V curves. Both the ZnO film and β-Ga_2O_3 film are about 100-nm thick. The distance between In electrodes is about 1 cm. The carrier concentration of the as-grown ZnO layer is $\sim 5\times10^{16}$ cm^{-3}. On the other hand, the β-Ga_2O_3 layer is highly electrically resistive (sheet resistance over 10^9 Ω). Thus no measurable conductivity was observed by the Hall measurement technique. The I–V curve of the β-Ga_2O_3/ZnO heterojunction presents an obvious rectifying property. The current increases sharply, presenting an on-state under an about 2-V positive bias and an off state under a reverse bias. The asymmetric ratio, $I(4\text{ V})/I(-4\text{ V})$, is over 10^5 as shown in the inset. Comparing with most other reports on Ga_2O_3-based heterojunctions, the asymmetry of I–V relation is very obvious in β-Ga_2O_3/ZnO heterojunction, indicating an excellent rectification characteristic. When the heterojunction is illuminated under 254-nm light, the photocurrent presents a pronounced increase from 247.25 μA to 364.58 μA at 5 V and 3.24 μA to 68.79 μA at −7 V. In contrast, the heterojunction is not sensitive to 365-nm light, indicating a solar-blind characteristic. The spectral responsivity (R_λ) is an important parameter to determine the sensitivity of the photodetector. A rejection ratio of R_λ value for 254 nm/365 nm is approximately 600 at −7-V bias.

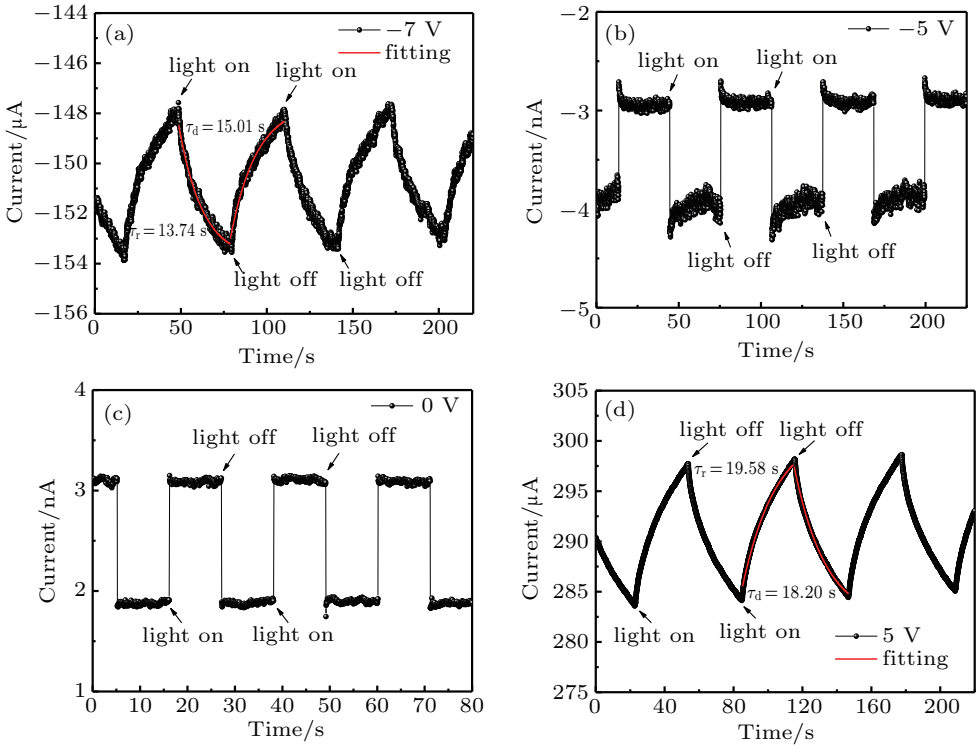


Fig. 3. Plots of time-dependent photoresponse of the β-Ga_2O_3/ZnO heterojunction under illumination of 254-nm wavelength light at different switching on/off bias voltages: (a) −7 V, (b) −5 V, (c) 0 V, and (d) 5-V bias.

The time-dependent photoresponse measurements are performed to evaluate the response speed of the photodetector by periodically turning the mercury lamp ON and OFF under different bias voltages (−7 V, −5 V, 0 V, and 5 V). The heterojunction exhibits robustness and good reproducibility performance, as the fluctuations in response curve are nearly identical and repeatable as shown in Fig. 3. The quantitative analysis of the current rise process and decay process are fitted by (involving the fitting of the time-dependent photoresponse curve) an exponential relaxation equation of the following type:

$$I = I_0 + A\,\mathrm{e}^{-t/\tau},$$

where I_0 is the steady-state current, A is constant, and τ is the relaxation time constant. The rise time constant τ_r and decay time constant τ_d are marked in the figure. At zero-bias, the dark current is approximately 1.89 nA. Under the illumination of 254-nm wavelength light with an intensity of 400 μW/cm^2, the current increases rapidly to a stable value of 3.12 nA, revealing the self-powered characteristic of the heterojunction. When the UV light turns off, the current decreases instantaneously down to the initial dark value. The rise time τ_r and the decay time τ_d at zero bias are approximately 0.035 s and 0.032 s, respectively. In contrast, the response times for applied bias of −5 V, −7 V, and 5 V are slower than that for zero bias, specifically, τ_r is 0.065 s and τ_d is 0.033 s at −5 V; τ_r is 19.58 s and τ_d is 18.20 s at 5 V; τ_r is 13.74 s and τ_d is 15.01 s at −7 V.

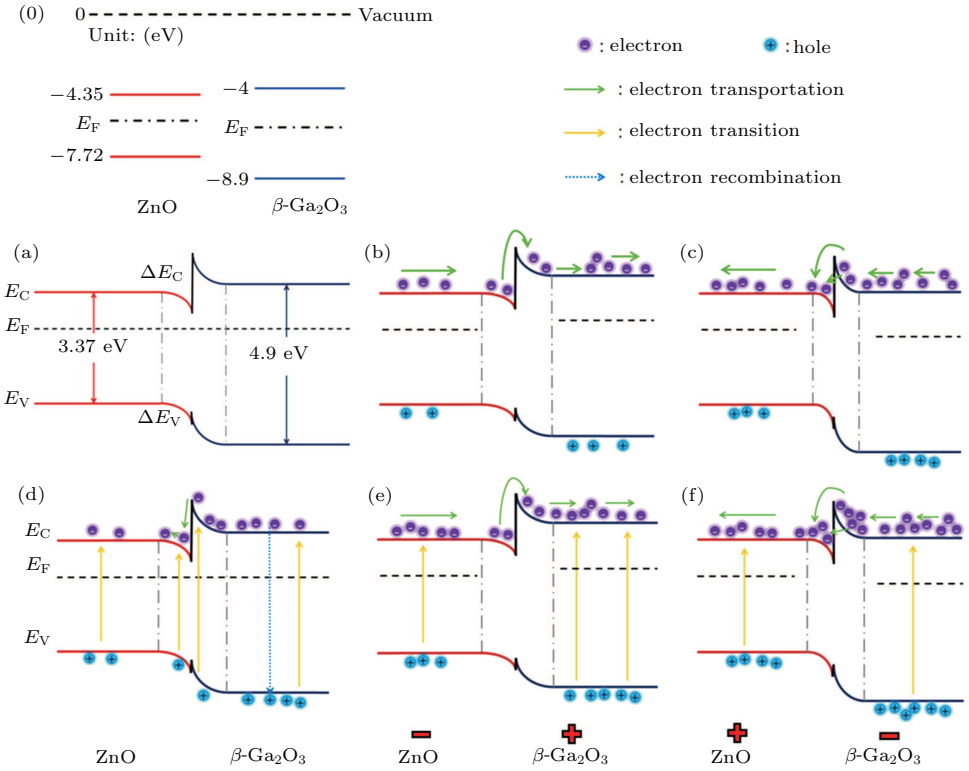


Fig. 4. Schematic energy band diagrams of β-Ga_2O_3/ZnO heterojunction. (0) Before contact. After contact under dark conditions at (a) 0 V bias, (b) reverse bias, and (c) positive bias; under 254-nm illumination at (d) 0 V bias, (e) reverse bias, and (f) positive bias.

The rectifying I–V and photoelectric characteristic of the heterojunction can be explained by the energy band diagram shown in Fig. 4. The photocurrent generation and transportation mechanism are considered by using the Anderson model. The band gap of β-Ga_2O_3 and ZnO are taken to be 4.9 eV and 3.37 eV, and the electron affinities are taken to be 4 eV and 4.35 eV respectively.[34,35] Fermi levels are raised up after β-Ga_2O_3 has contacted ZnO, and the electrons will flow from β-Ga_2O_3 to ZnO. The accumulation region will be formed in the ZnO layer, while the depletion region will be formed in the β-Ga_2O_3 layer. When the heterojunction is in thermal equilibrium, Fermi levels of β-Ga_2O_3 and ZnO are uniform. Herein, a built-in electric field near the interface would be built to balance electron drift, called the space charge region. When a reverse bias is applied, the electric field direction is consistent with the built-in electric field. As the field in the space charge region widens, the barrier of the conduction band between β-Ga_2O_3 and ZnO increases, and the electron energy will diminish and be insufficient to pass through the barrier. When a forward bias is applied, the space charge region narrows and the barrier of the conduction band between β-Ga_2O_3 and ZnO lowers, leading to the facilitation of electron transfers. Under 254-nm DUV light illumination, the electrons are excited to jump from valence band to conduction band and the photogenerated electron-hole pairs are separated by the built-in electric field. The carrier concentration in the space charge region increases, resulting in the increase of the photocurrent. The applied bias can conduce to separating more photogenerated electron-hole pairs, which leads to an increase for photogenerated carrier concentration. However, due to the presence of oxygen vacancies in β-Ga_2O_3 and ZnO thin films, the photogenerated electrons will be captured by oxygen vacancies. Therefore, the slow response can be attributed to the extremely slow carrier trapping and releasing process under applied voltage. At zero bias voltage, the original built-in electric field intensity is insufficient to offset the increasing photocarrier drift. The number of carriers in the space charge region is a small fraction due to its narrow width. Hence, the photocurrent at zero bias voltage is small. However, the carriers released from the oxygen vacancy traps make almost no contribution to the current under zero bias, thus resulting in a fast response.

4. Conclusions and perspectives

The β-Ga_2O_3/ZnO heterojunctions are fabricated on sapphire substrates by laser molecular beam epitaxy. The obtained heterojunction presents an excellent rectifying characteristic and solar-blind photoelectric property. At 0-V bias, the photodetector exhibits high response speed and high stability, revealing self-powered characteristics. The observed self-powered performance can be related to the built-in electric field driven photogenerated electron-hole pairs' separation in the depletion. An enhanced responsivity is obtained when the applied bias increases, owing to the increased electric field

promoting carrier separation. The film-type heterojunction has a low cost and extensive application prospect.

References

[1] Razeghi M and Rogalski A 1996 *J. Appl. Phys.* **79** 7433

[2] Guo D Y, Zhao X L, Zhi Y S, Cui W, Huang Y Q, An Y H, Li P G, Wu Z P and Tang W H 2016 *Mater. Lett.* **164** 364

[3] Li W H, Zhao X L, Zhi Y S, Zhang X H, Chen Z W, Chu X L, Yang H J, Wu Z P and Tang W H 2018 *Appl. Opt.* **57** 538

[4] Pei J N, Jiang D Y, Tian C G, Guo Z X, Liu R S, Sun L, Qin J M, Hou J H, Zhao J X, Liang Q C and Gao S 2015 *Acta Phys. Sin.* **64** 067802 (in Chinese)

[5] Zheng J J, Wang Y R, Yu K H, Xu X X, Sheng X X, Hu E T and Wei W 2018 *Acta Phys. Sin.* **67** 118502 (in Chinese)

[6] Li J J, Gao Z Y, Xue X W, Li H M, Deng J, Cui B F and Zou D S 2016 *Acta Phys. Sin.* **65** 118104 (in Chinese)

[7] Chen H Y, Liu K W, Hu L F, Al-Ghamdi A A and Fang X S 2015 *Mater. Today* **18** 493

[8] Brown D M, Fedison J B, Hibshman J R, Kretchmer J W, Lombardo L, Matocha K S and Sandvik P M 2005 *IEEE Sens. J.* **5** 983

[9] Vert A, Soloviev S and Sandvik P 2009 *Phys. Status Solidi* **206** 2468

[10] Jiang H, Egawa T and Ishikawa H 2006 *IEEE Photon. Technol. Lett.* **18** 1353

[11] Tut T, Gokkavas M, Inal A and Ozbay E 2007 *Appl. Phys. Lett.* **90** 163506

[12] Zhang W, Xu J, Ye W, Li Y, Qi Z Q, Dai J N, Wu Z H, Chen C Q, Yin J, Li J, Jiang H and Fang Y Y 2015 *Appl. Phys. Lett.* **106** 021112

[13] Zheng Q H, Huang F, Ding K, Huang J, Chen D G, Zhan Z B and Lin Z 2011 *Appl. Phys. Lett.* **98** 221112

[14] Fan M M, Liu K W, Chen X, Wang X, Zhang Z Z, Li B H and Shen D Z 2015 *Acs Appl. Mater. Inter.* **7** 20600

[15] Li P G, Shi H Z, Chen K, Guo D Y, Cui W, Zhi Y S, Wang S L, Wu Z P, Chen Z W and Tang W H 2017 *J. Mater. Chem. C* **5** 10562

[16] Oshima T, Okuno T, Arai N, Suzuki N, Ohira S and Fujita S 2008 *Appl. Phys. Express* **1** 011202

[17] Wu Z P, Bai G X, Qu Y Y, Guo D Y, Li L H, Li P G, Hao J H and Tang W H 2016 *Appl. Phys. Lett.* **108** 211903

[18] Guo D, Wu Z, Li P, An Y, Han L, Guo X, Hui Y, Wang G, Sun C and Li L 2014 *Opt. Mater. Express* **4** 1067

[19] Li Y, Tokizono T, Liao M, Miao Z, Koide Y, Yamada I and Delaunay J J 2010 *Adv. Funct. Mater.* **20** 3972

[20] Wang X, Chen Z W, Guo D Y, Zhang X, Wu Z P, Li P G and Tang W H 2018 *Opt. Mater. Express* **8** 2918

[21] Peng Y, Zhang Y, Chen Z, Guo D, Zhang X, Li P, Wu Z and Tang W 2018 *IEEE Photon. Technolnol. Lett.* **30** 993

[22] Liu, Z, Li, P G, Zhi, Y S, Wang, X L, Chu, X L and Tang W H 2019 *Chin. Phys. B* **28** 017105

[23] Sasaki K, Higashiwaki M, Kuramata A, Masui T and Yamakoshi S 2013 *IEEE Electron. Dev. Lett.* **34** 493

[24] Fan P, Chettiar U K, Cao L, Afshinmanesh F, Engheta N and Brongersma M L 2012 *Nat. Photon.* **6** 380

[25] Qu Y Y, Wu Z P, Ai M L, Guo D Y, An Y H, Yang H J, Li L H and Tang W H 2016 *J. Alloy. Compd.* **680** 247

[26] An Y H, Guo D Y, Li S Y, Wu Z P, Huang Y Q, Li P G, Li L H and Tang W H 2016 *J. Phys. D: Appl. Phys.* **49** 285111

[27] Feng W, Wang X, Zhang J, Wang L, Zheng W, Hu P, Cao W and Yang B J 2014 *J. Mater. Chem. C* **2** 3254

[28] Guo D Y, Su Y, Shi H Z, Li P G, Zhao N, Ye J H, Wang S L, Liu A P, Chen Z W, Li C R and Tang W H 2018 *ACS Nano* **12** 12827

[29] Guo D Y, Li P G, Chen Z W, Wu Z P and Tang W H 2019 *Acta Phys. Sin.* **68** 078501 (in Chinese)

[30] Guo X C, Hao N H, Guo D Y, Wu Z P, An Y H, Chu X L, Li L H, Li P G, Lei M and Tang W H 2016 *J. Alloys Compd.* **660** 136

[31] Guo D, Liu H, Li P, Wu Z, Wang S, Cui C, Li C and Tang W 2017 *ACS Appl. Mater. Interfaces* **9** 1619

[32] Wu Z P, Jiao L, Wang X L, Guo D Y, Li W H, Li L H, Huang F and Tang W H 2017 *J. Mater. Chem. C* **5** 8688

[33] Zhao B, Fei W, Chen H, Wang Y, Jiang M, Fang X and Zhao D 2015 *Nano Lett.* **15** 3988

[34] Zhang L, Li Q, Shang L, Zhang Z, Huang R and Zhao F J 2012 *J. Phys. D: Appl. Phys.* **45** 485103

[35] Guo D Y, Wu Z P, An Y H, Guo X C, Chu X L, Sun C L, Li L H, Li P G and Tang W H 2014 *Appl. Phys. Lett.* **105** 023507